



Selective proteasome degradation of C-terminally-truncated human WFS1 in pancreatic beta cells

Hiraku Tokuma¹, Daisuke Sakano¹, Katsuya Tanabe² , Yukio Tanizawa², Nobuaki Shiraki¹ and Shoen Kume¹ 

¹ School of Life Science and Technology, Tokyo Institute of Technology, Yokohama, Japan

² Division of Endocrinology, Metabolism, Haematological Science and Therapeutics, Yamaguchi University Graduate School of Medicine, Ube, Japan

Keywords

beta cells; degradation; diabetes; endocrine; proteasome; WFS1

Correspondence

S. Kume and D. Sakano, School of Life Science and Technology, Tokyo Institute of Technology, 4259-B-25 Nagatsuta-cho, Midori-ku, Yokohama, Kanagawa 226-8501, Japan

E-mails: skume@bio.titech.ac.jp (SK); dsakano@bio.titech.ac.jp (DS)

Wolfram syndrome is a monogenic disease mainly caused by mutations in the *WFS1* gene. Mutations in the *WFS1* gene give rise to diabetes. Here, we characterized mutant WFS1 proteins by studying the stability of full-length wild-type (WT) WFS1, a missense mutant P724L, and two C-terminally truncated mutants, W837X and Y652X. We compared their stability by overexpressing them in MIN6 and HEK293T cells. The C-terminally truncated mutants W837X and Y652X are degraded more rapidly than the missense P724L mutant or wild-type WFS1 in MIN6 cells. In contrast, Y652X is more stable than WT or other mutant WFS1 proteins in HEK293T. In conclusion, we found that C-terminally truncated WFS1 mutants are selectively degraded in a cell type-specific manner.

(Received 17 March 2023, revised 28 June 2023, accepted 11 July 2023)

doi:10.1002/2211-5463.13674

Edited by Alberto Alape-Girón

Wolfram Syndrome is an autosomal recessive disorder characterized by early-onset insulin-dependent diabetes mellitus optic atrophy and progressive neurodegeneration [1]. The *WFS1* gene is identified as the main locus mutated in the majority of the patients [2,3]. Wolfram syndrome is characterized as a spectrum disorder. More than 200 different variations in the *WFS1* gene have been described in Wolfram syndrome patients [4–7]. *WFS1* encodes a transmembrane protein, also called wolframin, which consists of 890 amino acids and is predicted to have 9 or 10 membrane-spanning domains. The WFS1 protein is ubiquitously expressed

but at higher levels in the brain, heart, lung, and pancreas [2,3].

WFS1 is localized predominantly in the endoplasmic reticulum (ER) membrane [8] and appears to be enriched in mitochondria-associated ER membranes (MAMs). Although the endogenous functions of WFS1 remain unclear, previous studies have pointed out the involvement of WFS1 in ER stress regulation and Ca²⁺ homeostasis [9–12]. Recent studies revealed a role of WFS1 in regulating mitochondrial Ca²⁺ transfer through the MAMs [13–16].

Abbreviations

DAPI, 4',6-diamidino-2-phenylindole; ER, endoplasmic reticulum; HEK, human embryonic kidney cells; HRP, horseradish peroxidase; hWFS1, human WFS1; MAMs, mitochondria-associated ER membranes; MIN6, mouse insulinoma 6; ROI, region of interest; SD, standard deviation; TCID50, median tissue culture infectious dose; WFS1, Wolfram syndrome 1; WT, wild-type.

Mutations in the *WFS1* gene are reported to affect the WFS1 protein stability [17–19]. *Wfs1*-knockout mice were developed [20–22], which exhibit enhanced ER stress, impaired insulin processing and regulation of insulin secretion and develop progressive glucose intolerance and increased pancreatic beta cell death.

Previous studies of genotype–phenotype correlations for WFS1 mutations in Japanese Wolfram syndrome patients revealed that WFS1 mutation could be subdivided into groups in correlation with clinical severity. Variants with nonsense mutations, frameshift mutations, and/or multiple amino acid insertion/deletions in both alleles show more severe symptoms than variants with missense mutations and/or single amino acid insertions in both alleles [7].

In the present study, we introduced one missense and two nonsense mutations in the *WFS1* cDNA to gain insights into the relationship between the severity of the mutations. We overexpressed the wild-type (WT) and mutant WFS1 cDNAs and compared their stabilities in mouse insulinoma 6 (MIN6) cells, a mouse pancreatic β -cell line, and HEK293T cells, a human embryonic kidney cell line.

Materials and methods

Cell lines

MIN6 cells were obtained from J. Miyazaki in Osaka University and HEK293T cells were from RIKEN BioResource Center (BRC) [23,24].

WFS1 mutant adenovirus vector construction

A cDNA fragment of human WFS1 WT open reading frame (nt. 1–2673; NP_005996.1 aa: 1–890) was cloned from human islet cDNA by PCR. Human WFS1 mutants were generated using inverse PCR and In-Fusion HD (Takara Bio Inc., Shiga, Japan). Human WFS1 was used as the template for PCR. All primers for inverse PCR are listed in Table S1. The WFS1 mutant adenoviral vectors are registered at GenBank and listed in Table S2. Adenoviruses were produced as described [25]. Adenovirus titers were determined by Median Tissue Culture Infectious Dose (TCID₅₀) [26].

HaloTag pulse-chase assay

MIN6, HEK293T cells were cultured in Dulbecco's modified Eagle's medium supplied with 25 mM glucose (Thermo Fisher Scientific Inc., Waltham, MA, USA), 10% fetal bovine serum, 100 μ M non-essential amino acids, 2 mM L-glutamine, 50 units·mL⁻¹ penicillin, 50 μ g·mL⁻¹ streptomycin, and 100 μ M 2-mercaptoethanol, at 37 °C, 5% CO₂. Cells were dissociated with 0.05% Trypsin–EDTA (Thermo Fisher

Scientific) and seeded on a 96-well plate coated with Easy iMatrix-511 (Matrixome Inc., Osaka, Japan) at a density of 50 000 cells per well (MIN6 cells) or 10 000 cells (HEK293T cells). MIN6 cells were infected with adenovirus carrying *HaloTag-hWFS1* or *hWFS1* mutants to examine the steady state of the protein expression in Fig. 1 and in the pulse-labeling experiment in Fig. 2. The multiplicity of infection was 3.3. In the pulse-chase experiment, *HaloTag-hWFS1* or mutants were inserted into the pCAGGS vector [27] and transfected using Lipofectamine 3000 (Thermo Fisher Scientific) in Figs 3 (MIN6) and 4 (HEK293T). *HaloTag-hWFS1* overexpressing vectors are registered at GenBank and listed in Table S2. Labeling using R110 or TMR was done following the manufacturer's protocol. After infection or transfection, cells were cultured for 32 h, then treated with HaloTag R110Direct™ ligand (R110; Promega, Madison, WI, USA) for 16 h to bind to the already produced 'old' HaloTag-hWFS1. After washing with medium to remove the R110, cells were cultured in the presence of a proteasome inhibitor, MG132 (10 μ M, in the pulse-chase experiment), or control DMSO (in the pulse labeling). Then, cells were treated with HaloTag TMR ligand (TMR; Promega) for 15 min (\pm MG132) to label newly synthesized HaloTag-hWFS1. After pulse labeling with TMR, the steady-state expression levels of the WFS1 proteins were examined after fixing the cells in 4% paraformaldehyde in PBS and counter-stained with DAPI (F. Hoffmann-La Roche Ltd., Basel, Switzerland) (Fig. 2). R110 or TMR fluorescence that labeled the HaloTag-hWFS1 in the cells was analyzed with ImageXpress Micro Confocal High-Content Imaging System and MetaXpress (Molecular Devices, San Jose, CA, USA). To chase the TMR-labeled HaloTag WT or mutant hWFS1 proteins, cells were counter-stained with Hoechst 33342 (Bio-Rad Laboratories Inc., Richmond, CA, USA) and cultured for 8, 16, or 24 h in the absence of MG132 (Figs 3 and 4). The areas of cells expressing the WFS1 proteins were determined as region of interest (ROI) based on the 0 h image labeled with R110. The averaged TMR fluorescence intensity values were obtained for each ROI at 0, 8, 16, and 24 h after TMR treatment. All calculations were performed using the IMAGE J FIJI program [28] for images taken by IMAGEXPRESS.

Western blot analysis

Cells were lysed with 2 \times Laemmli buffer [0.1 mM Tris–HCl (pH 6.8), 4% SDS, 20% Glycerol, 1.7 M 2-mercaptoethanol] or with loading buffer [62.5 mM Tris–HCl (pH 6.8), 2% SDS, 10% glycerol and 41.6 mM dithiothreitol] and sonicated for 20 s, and incubated overnight at 55 °C. Samples were separated using an 8% acrylamide gel and transferred onto a polyvinylidene difluoride membrane (Merck Millipore Ltd, Billerica, MA, USA) and incubated overnight at 4 °C with mouse anti-HaloTag (1 : 1000, Cat: G9211; Promega), rabbit anti-WFS1 (1 : 1000) [29], or mouse anti- α -tubulin (1 : 2000, Cat: T6074; Sigma, Billerica, MA, USA). After

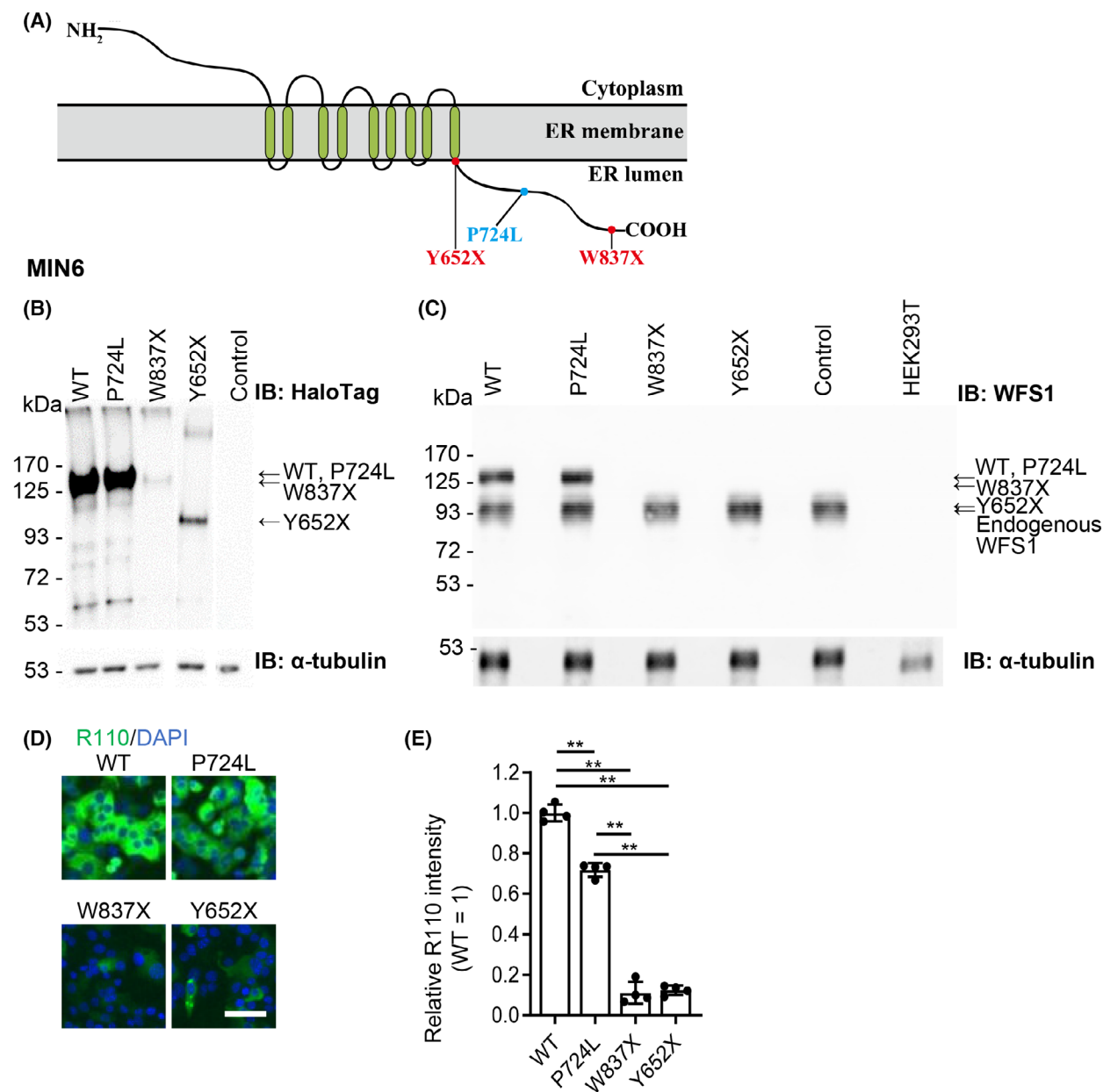


Fig. 1. The C-terminal deleted hWFS1 mutants are unstable in MIN6 cells. (A) A schematic drawing of the structure of the hWFS1 protein. Mutations indicated in red are nonsense or frameshift mutations. The Mutation indicated in blue is a missense mutation. (B, C) Whole-cell lysates from MIN6 cells infected with adenovirus carrying HaloTag-hWFS1 (WT, P724L, W837X, and Y652X), uninfected MIN6 cells (Control), and HEK293T cells were immunoblotted with anti-HaloTag (B, upper panel), anti-WFS1 (C, upper panel) or anti- α -tubulin antibody as internal controls (B, C lower panels). The steady-state protein levels of C-terminal deleted mutant hWFS1 (W837X, Y652X) were expressed at lower levels than HaloTag-hWFS1 WT or P724L (B). The exogenous HaloTag-hWFS1 WT or P724L were expressed at similar levels to the endogenous WFS1 (C). (D, E) Fluorescent images of the Halo ligand R110 labeled HaloTag-hWFS1 WT or mutants in MIN6 cells (D). The relative intensities of fluorescence of R110 labeled HaloTag-hWFS1 WT or mutant versus the WT WFS1 (=1) are shown (E). $N = 4$. (D) Scale bar = 50 μ m. Data are presented as scattered plots with the means \pm SD. Significant differences are shown as ** $P < 0.01$, by one-way ANOVA and Dunnett multiple comparisons test.

washing with PBST (PBS containing 0.1% Tween20), the membrane was probed with a horseradish peroxidase-conjugated antibody. The membrane was scanned using

FUSION-SOLO.4S.WL (M&S Instruments Inc., Tokyo, Japan) after reacting with Luminata Forte Western HRP Substrate (Merck Millipore).

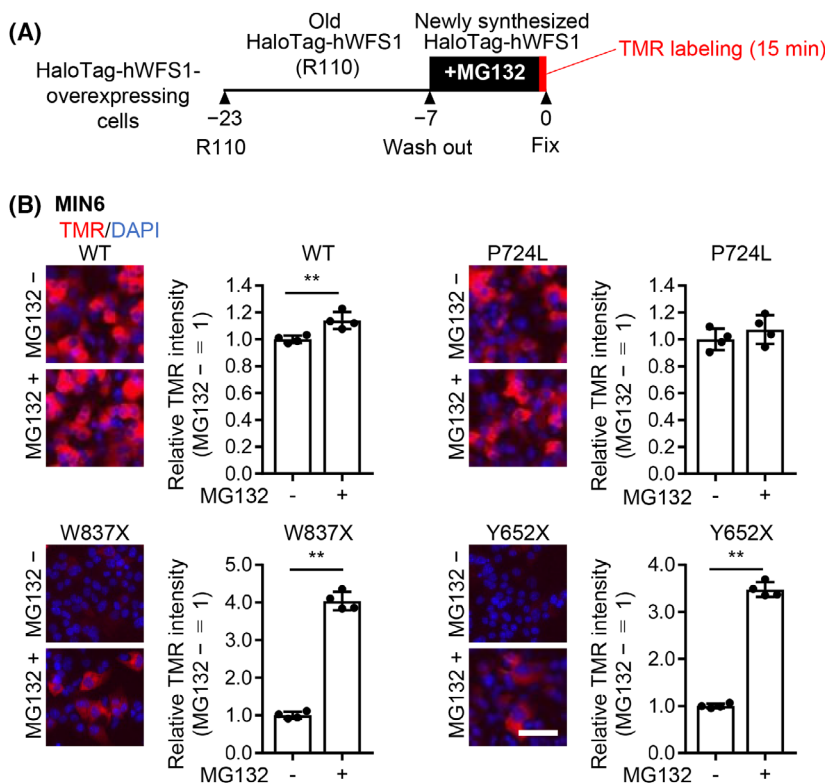


Fig. 2. C-terminally truncated hWFS1 proteins are degraded by the proteasome in MIN6 cells. (A) A schematic drawing of the pulse-labeling with TMR using the HaloTag system. HaloTag-hWFS1 overexpressing cells were incubated with R110 for 16 h to label the already produced 'old' HaloTag-hWFS1. Then the cells were incubated for 7 h with or without MG132, then labeled the newly synthesized HaloTag-hWFS1 with TMR. (B) Left panels: representative TMR fluorescence images of MIN6 cells. Right panels: relative average TMR intensities immediately after TMR labeling of the HaloTag-hWFS1 proteins accumulated in MIN6 cells. Proteasome inhibitor MG132 promoted the accumulation of the WT WFS1 to 1.1-fold and C-terminally truncated HaloTag-hWFS1 to 4.0-fold (W837X) or 3.5-fold (Y652X), versus without MG132. In contrast, MG132 did not promote the accumulation of the missense mutant (P724L). $N = 4$. Data are presented as scattered plots with the mean \pm SD. Significant differences are shown as ** $P < 0.01$, by Student's t -test. Scale bar = 50 μ m.

Statistics

Data are presented as mean \pm SD (standard deviation) with individual data. Data were analyzed by one-way ANOVA and Dunnett multiple comparisons test (Fig. 1D), Student's t -test (Fig. 2B), or Mann-Whitney's U -test (Figs 3C and 4B). Significant differences are shown as ** $P < 0.01$ or $P < 0.05$ in the tables. All data were obtained from more than three independent experiments except those specifically indicated.

Results

The hWFS1 C-terminally truncated mutants are unstable in MIN6 cells

We investigated one missense and two C-terminally truncated human *WFS1* (*hWFS1*) mutations. The missense mutation corresponds to the luminal C-terminal

(P724L), and the C-terminal truncation mutations Y652X and W837X lead to the truncation of a large portion of the C-terminus end (Y652X) or truncation of the last 54 amino acid residues (W837X) (Fig. 1A). The patients with the P724L mutation were previously described as late onsets of diabetes mellitus, compared to those with the W837X and Y652X mutations, who developed early onset diabetes [7].

To assess the steady-state expression of the hWFS1 mutants, we generated adenoviral vectors carrying human WT or mutant hWFS1 tagged with HaloTag [30] at their N-terminal ends. We infected the MIN6 cell with the above adenoviral vectors and detected by western blot analysis using an anti-HaloTag antibody or anti-WFS1 antibody. The exogenous HaloTag WFS1 WT or the missense hWFS1 mutant P724L gave strong signals at approximately 134 kDa. In contrast, the C-terminally truncated hWFS1 mutants Y652X and W837X expressed in MIN6 cells gave

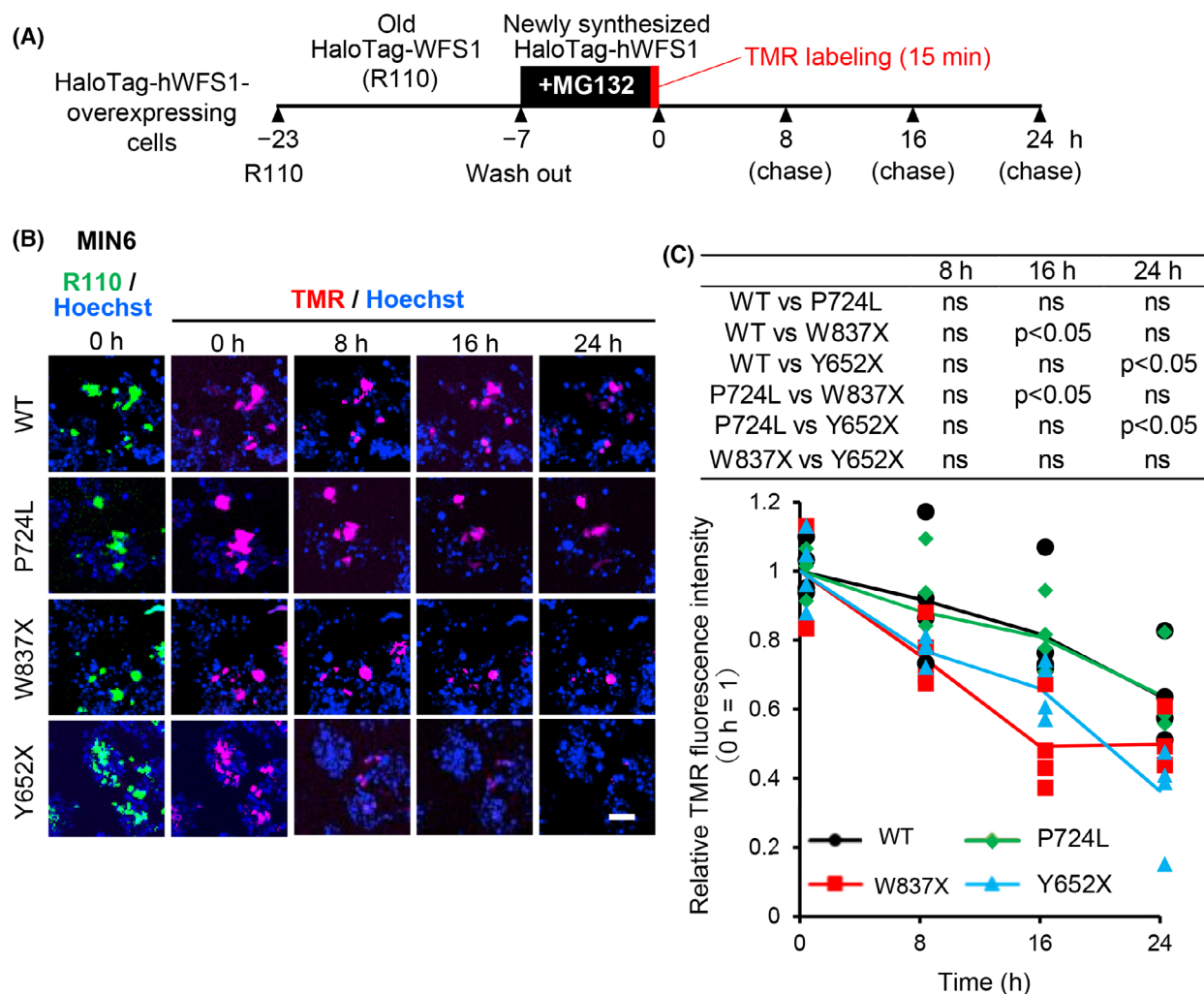


Fig. 3. C-terminally truncated W837X, and Y652X proteins are rapidly degraded in MIN6 cells. (A) A schematic drawing of the pulse-chase experiment using the HaloTag system. HaloTag-hWFS1 overexpressing cells incubated with R110 for 16 h (R110 labeled old hWFS1) were incubated with MG132 for 7 h, then labeled for 15 min with TMR (new hWFS1) and chased for the indicated times in the absence of MG132. (B) Representative time-dependent TMR fluorescence images of WT or mutant WFS1 overexpressing MIN6 cells chased for 0, 8, 16, and 24 h. Scale bar = 50 μ m. (C) R110 fluorescence of WT or mutant WFS1 protein expressing MIN6 cells, used for determining the ROIs. Time-dependent average TMR fluorescence intensities of WT or mutant WFS1 in the pulse-chase experiment in (B). Each point represents the average intensity of the ROI in each image. Cells were counter-stained with Hoechst. The fluorescence intensities are expressed as fold-change versus the WT or mutant WFS1 at 0 h, respectively. C-terminally truncated WFS1 proteins were degraded more rapidly than full-length WT and missense mutant P724L. $N = 4$. Data are presented as scattered plots with the mean \pm SD. Significant differences were analyzed by Mann–Whitney's U -test and are shown in a table. $P < 0.05$; ns, not significant.

weak signals at 127.7 kDa (W837X) or 106.8 kDa (Y652X) (Fig. 1B). In MIN6 cells, the exogenous HaloTag WFS1 WT and P724L were expressed at almost similar levels with those of the endogenous WFS1, detected by an anti-WFS1 antibody (Fig. 1C). In W837X and Y652 overexpressed MIN6 cells, the endogenous WFS1 bands were also detected, although the overexpressed HaloTag-W837X or Y652X were undetectable (Fig. 1C).

We also used a synthetic Halo ligand R110 that binds to the HaloTag-hWFS1 protein. The R110 fluorescence visualizes the expression of the WT or mutant WFS1 (Fig. 1D,E). Representative images are shown in Fig. 1D. Average fluorescence intensities in the ROIs are shown in scattered plots (Fig. 1E). The results revealed that the P724L missense mutation was expressed at approximately 0.7-fold of that of the WT. The C-terminally truncated mutants W837X and Y652X

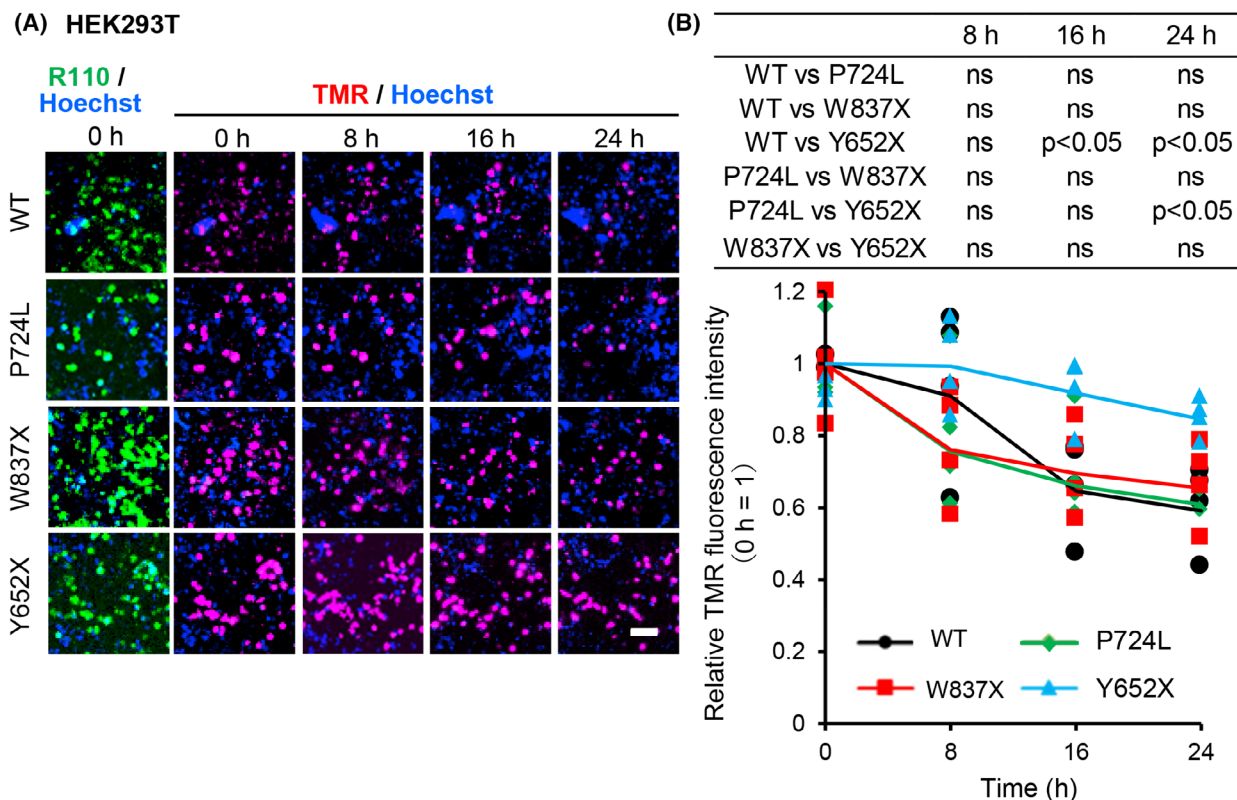


Fig. 4. C-terminally truncated Y652X mutant is more stable than WT, P724L or W837X hWFS1 in HEK293T cells. (A) HEK293T cells overexpressing HaloTag-hWFS1 WT or mutants by adenovirus infection were treated similarly, with the old hWFS1 proteins labeled with R110, then incubated with MG132 for 7 h, then labeled for 15 with TMR to label new hWFS1 and chased for the indicated times in the absence of MG132. Representative time-dependent TMR fluorescence images of HaloTag-hWFS1 WT or mutant overexpressing HEK293T cells chased for 0, 8, 16, and 24 h. Cells were counter-stained with Hoechst. Scale bar = 50 μ m. (B) R110 fluorescence of WT or mutant WFS1 protein expressing HEK293T cells, used for determining the ROIs. Time-dependent average TMR fluorescence intensities of HaloTag-hWFS1 WT or mutants in the pulse-chase experiment in HEK293T cells. Each point represents the average intensity of each image. The fluorescence intensities are expressed as fold-change versus the WT or mutant WFS1 at 0 h, respectively. $N = 4$. Data are presented as scattered plots with the mean \pm SD. Significant differences were analyzed by Mann–Whitney’s U -test and are shown in a table. $P < 0.05$; ns, not significant.

were expressed at 0.1-fold of the WT (Fig. 1D,E). The results suggest an instability of the C-terminally truncated hWFS1 mutations expressed in MIN6 cells.

C-terminally truncated hWFS1 proteins are rapidly degraded by the proteasome in MIN6 cells

It is reported that WFS1 mutants are degraded by the ubiquitin-proteasome system [17,18]. We investigate whether the instability of the WFS1 mutant proteins expressed in MIN6 cells is through proteasome degradation. After labeling the already produced ‘old’ HaloTag-hWFS1 with R110, the HaloTag-hWFS1 overexpressing MIN6 cells were incubated for 7 h with or without proteasome inhibitor MG132, then labeled the newly synthesized HaloTag-hWFS1

protein with TMR ligand (Fig. 2A, pulse labeling with TMR). The results showed that TMR-labeled WT and P724L mutant hWFS1 protein accumulated even without MG132. MG132 treatment increased the accumulation of WT or P724L hWFS1 to about 1.1-fold versus the untreated group (Fig. 2B, right). In contrast, the C-terminally truncated hWFS1 mutants were detected at low levels in the absence of MG132. In the presence of MG132, the C-terminally truncated mutants W837X or Y652X accumulated up to approximately 4.0-fold (W837X) or 3.5-fold (Y652X) in MIN6, compared to without MG132 (Fig. 2B).

Adding MG132 rescued the degradation of the C-terminally truncated mutants, indicating the proteasome-mediated mechanism is involved. To analyze this in detail, we performed another pulse-chase

labeling experiment (Fig. 3A). The R110-labeled HaloTag-hWFS1 expressing MIN6 cells (overlapped with the TMR-labeled cells) (0 h) were used to determine the ROIs. TMR-labeled HaloTag-hWFS1 proteins were chased for 8, 16, and 24 h. As a result, WT and P724L proteins were reduced to about 0.65-fold after incubating without MG132 for 24 h. In contrast, C-terminally truncated mutants W837X and Y652X were rapidly degraded to about 0.40- to 0.50-fold at 16 h (W837X) or 24 h (Y624X) in MIN6 cells (Fig. 3B,C).

The results indicate a proteasome-mediated rapid degradation of C-terminally truncated mutants W837X and Y652X in MIN6 cells.

C-terminally truncated mutant Y652X is more stable in HEK293T cells compared to WT or other WFS1 mutants

We then examined the stability of WT and mutants in HEK293T cells. We performed similar pulse-chase experiments in HEK293T cells. HEK293T cells expressed WFS1 endogenously at a much lower level than MIN6 cells (Fig. S1). The newly synthesized HaloTag-WT or mutant hWFS1 proteins expressed in the HEK293T cells were labeled with TMR (pulse, 0 h) and were chased for 8, 16, and 24 h in the absence of MG132.

Without MG132, the WT and the missense P724L mutant were degraded to approximately 0.60-fold (Fig. 4A,B), and the C-terminally truncated mutant W837X was about 0.65-fold at 24 h. In contrast, the C-terminally truncated mutant Y652X was about 0.85-fold at 24 h. The results indicate that the C-terminally truncated Y652X mutant is the most stable form in HEK293T cells compared to the WT or the P724L mutant (Fig. 4A,B).

Discussions

We compared the stability of WT and mutant WFS1 protein in MIN6 and HEK293T cells. The C-terminus truncated mutants W652X and W837X are degraded by the proteasome pathway in MIN6 cells. In contrast, the C-terminally truncated mutant W652X is more stable than WT or other WFS1 mutants in HEK293T cells. MG132 treatment did not restore the C-terminally truncated mutants to accumulate to the WT level, suggesting the involvement of other non-proteasomal mechanisms. The result suggests that protein stability depends on the tissue or cell environment, which agrees that protein stability varies among tissues [31].

Our results agree with a previous report that the C-terminally truncated mutants exhibited higher stabilities than the WT WFS1 in HEK293T cells [18]. However, the exact mutants used between ours and the previous studies differ. Notably, WT and mutant WFS1 seem to accumulate at similar levels at a steady state in HEK293T cells [18], which agrees with our present results. In MIN6 cells, the steady-state accumulations of C-terminus truncated mutants W837X and T652X were approximately 0.1-fold of the WT WFS1 protein, which was much lower compared to HEK293T cells. The results indicate that WFS1 WT and mutants are more stable in HEK293T than in MIN6 cells. A selective degrading mechanism of C-truncated WFS1 mutants seems to exist in beta cells. In MIN6 cells, the endogenous WFS1 was not degraded by overexpressing W837X or Y652X mutants, thereby confirming that the degradation system was not activated. The discrepancies between the stability of the WT and mutant WFS1 in MIN6 and HEK293T cells might be due to the different expression levels in regulating proteins involved in the degradation processes in a cell type-specific manner, which remains to be elucidated.

It is reported that the HECT-type ligase ubiquitin ligase (E3) Smad ubiquitination regulatory factor 1 (Smurf1) binds to the C-terminus of WFS1 and degrades WFS1 thus contributing to the instability in HEK293T cells [18]. However, the C-terminally truncated WFS1 mutants are unstable in MIN6 cells, suggesting a selective degrading mechanism of C-terminally truncated WFS1 mutants in beta cells. Expression of other members of the E3 ubiquitin ligase or other targeted protein degrading mechanisms, such as ERAD or SUMOylation, are reported in the pancreatic beta cells and might take part in regulating protein stability. However, we did not find any motif existing in the WFS1 protein [10,32–37].

Understanding the molecular mechanism regulating WFS1 stability might provide a potential therapeutic target for Wolfram syndrome.

Acknowledgements

We thank the members of the Animal Centers and Biomaterials Analysis Division, Open Facility Center, and Open Research Facilities for Life Science and Technology at the Tokyo Institute of Technology for their technical assistance. This work was supported by Grants-in-Aid from the Ministry of Education, Culture, Sports, Science and Technology, Japan (#21H02978 to SK and #20K08325 to DS, #19H03710 to YT, and #20K08887 to KT). This work was also

supported in part by the Takeda Science Foundation, Japan Insulin Dependent Diabetes Mellitus (IDDM) Network.

Conflict of interest

The authors declare no conflict of interest.

Author contributions

HT performed the experiments, collected, analyzed, and discussed the data. DS discussed the data and provided conceptual input and technical advice. KT, YT, and NS discussed the data and gave technical advice. SK provided conceptual input, discussion, writing, and revision of the manuscript; approved the final version of the manuscript; and obtained funding.

Peer review

The peer review history for this article is available at <https://www.webofscience.com/api/gateway/wos/peer-review/10.1002/2211-5463.13674>.

Data accessibility

The data supporting this study's findings are openly available in GenBank at <https://www.ncbi.nlm.nih.gov/genbank/>, and the accession numbers are listed in Table S2.

References

- 1 Wolfram DJ and Wagener HP (1938) Diabetes mellitus and simple optic atrophy among siblings: report of four cases. *Mayo Clin Proc* **13**, 715–718.
- 2 Inoue H, Tanizawa Y, Wasson J, Behn P, Kalidas K, Bernal-Mizrachi E, Mueckler M, Marshall H, Donis-Keller H, Crock P *et al.* (1998) A gene encoding a transmembrane protein is mutated in patients with diabetes mellitus and optic atrophy (Wolfram syndrome). *Nat Genet* **20**, 143–148.
- 3 Strom TM, Hörtnagel K, Hofmann S, Gekeler F, Scharfe C, Rabl W, Gerbitz KD and Meitinger T (1998) Diabetes insipidus, diabetes mellitus, optic atrophy and deafness (DIDMOAD) caused by mutations in a novel gene (wolframin) coding for a predicted transmembrane protein. *Hum Mol Genet* **7**, 2021–2028.
- 4 Cryns K, Sivakumaran TA, Van den Ouweland JMW, Pennings RJE, Cremers CWRJ, Flothmann K, Young TL, Smith RJH, Lesperance MM and Van Camp G (2003) Mutational spectrum of the WFS1 gene in Wolfram syndrome, nonsyndromic hearing impairment, diabetes mellitus, and psychiatric disease. *Hum Mutat* **22**, 275–287.
- 5 De Heredia ML, Clères R and Nunes V (2013) Genotypic classification of patients with Wolfram syndrome: insights into the natural history of the disease and correlation with phenotype. *Genet Med* **15**, 497–506.
- 6 De Franco E, Flanagan SE, Yagi T, Abreu D, Mahadevan J, Johnson MB, Jones G, Acosta F, Mulaudzi M, Lek N *et al.* (2017) Dominant ER stress-inducing WFS1 mutations underlie a genetic syndrome of neonatal/infancy-onset diabetes, congenital sensorineural deafness, and congenital cataracts. *Diabetes* **66**, 2044–2053.
- 7 Matsunaga K, Tanabe K, Inoue H, Okuya S, Ohta Y, Akiyama M, Taguchi A, Kora Y, Okayama N, Yamada Y *et al.* (2014) Wolfram syndrome in the Japanese population; molecular analysis of wfs1 gene and characterization of clinical features. *PLoS One* **9**, e106906.
- 8 Takeda K, Inoue H, Tanizawa Y, Matsuzaki Y, Oba J, Watanabe Y, Shinoda K and Oka Y (2001) WFS1 (Wolfram syndrome 1) gene product: predominant subcellular localization to endoplasmic reticulum in cultured cells and neuronal expression in rat brain. *Hum Mol Genet* **10**, 477–484.
- 9 Fonseca SG, Fukuma M, Lipson KL, Nguyen LX, Allen JR, Oka Y and Urano F (2005) WFS1 is a novel component of the unfolded protein response and maintains homeostasis of the endoplasmic reticulum in pancreatic β -cells. *J Biol Chem* **280**, 39609–39615.
- 10 Fonseca SG, Ishigaki S, Osowski CM, Lu S, Lipson KL, Ghosh R, Hayashi E, Ishihara H, Oka Y, Permutt MA *et al.* (2010) Wolfram syndrome 1 gene negatively regulates ER stress signaling in rodent and human cells. *J Clin Invest* **120**, 744–755.
- 11 Osman AA, Saito M, Makepeace C, Permutt MA, Schlesinger P and Mueckler M (2003) Wolframin expression induces novel ion channel activity in endoplasmic reticulum membranes and increases intracellular calcium. *J Biol Chem* **278**, 52755–52762.
- 12 Takei D, Ishihara H, Yamaguchi S, Yamada T, Tamura A, Katagiri H, Maruyama Y and Oka Y (2006) WFS1 protein modulates the free Ca²⁺ concentration in the endoplasmic reticulum. *FEBS Lett* **580**, 5635–5640.
- 13 Cagalinec M, Liiv M, Hodurova Z, Hickey MA, Vaarmann A, Mandel M, Zeb A, Choubey V, Kuun M, Safiulina D *et al.* (2016) Role of mitochondrial dynamics in neuronal development: mechanism for Wolfram syndrome. *PLoS Biol* **14**, 1–28.
- 14 Angebault C, Fauconnier J, Patergnani S, Rieusset J, Danese A, Affortit CA, Jagodzinska J, Mégy C, Quiles M, Cazevielle C *et al.* (2018) ER-mitochondria cross-talk is regulated by the Ca²⁺ sensor NCS1 and is

- impaired in Wolfram syndrome. *Sci Signal* **11**, eaaq1380.
- 15 Zatyka M, Da Silva XG, Bellomo EA, Leadbeater W, Astuti D, Smith J, Michelangeli F, Rutter GA and Barrett TG (2015) Sarco(endo)plasmic reticulum atpase is a molecular partner of wolfram syndrome 1 protein, which negatively regulates its expression. *Hum Mol Genet* **24**, 814–827.
 - 16 Fischer TT and Ehrlich BE (2020) Wolfram syndrome: a monogenic model for diabetes mellitus and neurodegeneration. *Curr Opin Physiol* **17**, 115–123.
 - 17 Hofmann S and Bauer MF (2006) Wolfram syndrome-associated mutations lead to instability and proteasomal degradation of wolframin. *FEBS Lett* **580**, 4000–4004.
 - 18 Guo X, Shen S, Song S, He S, Cui Y, Xing G, Wang J, Yin Y, Fan L, He F *et al.* (2011) The E3 ligase Smurf1 regulates Wolfram syndrome protein stability at the endoplasmic reticulum. *J Biol Chem* **286**, 18037–18047.
 - 19 Yamaguchi S, Ishihara H, Tamura A, Yamada T, Takahashi R, Takei D, Katagiri H and Oka Y (2004) Endoplasmic reticulum stress and N-glycosylation modulate expression of WFS1 protein. *Biochem Biophys Res Commun* **325**, 250–256.
 - 20 Ishihara H, Takeda S, Tamura A, Takahashi R, Yamaguchi S, Takei D, Yamada T, Inoue H, Soga H, Katagiri H *et al.* (2004) Disruption of the WFS1 gene in mice causes progressive β -cell loss and impaired stimulus – secretion coupling in insulin secretion. *Hum Mol Genet* **13**, 1159–1170.
 - 21 Luuk H, Plas M, Raud S, Innos J, Sütt S, Lasner H, Abramov U, Kurrikoff K, Kõks S and Vasar E (2009) Wfs1-deficient mice display impaired behavioural adaptation in stressful environment. *Behav Brain Res* **198**, 334–345.
 - 22 Riggs AC, Bernal-Mizrachi E, Ohsugi M, Wasson J, Fatrai S, Welling C, Murray J, Schmidt RE, Herrera PL and Permutt MA (2005) Mice conditionally lacking the Wolfram gene in pancreatic islet beta cells exhibit diabetes as a result of enhanced endoplasmic reticulum stress and apoptosis. *Diabetologia* **48**, 2313–2321.
 - 23 Miyazaki JI, Araki K, Yamato E, Ikegami H, Asano T, Shibasaki Y, Oka Y, Yamamura KI and Miyazaki JI (1990) Establishment of a pancreatic β cell line that retains glucose-inducible insulin secretion: special reference to expression of glucose transporter isoforms. *Endocrinology* **127**, 126–132.
 - 24 Graham FL, Smiley J, Russell WC and Nairn R (1977) Characteristics of a human cell line transformed by DNA from human adenovirus type 5. *J Gen Virol* **36**, 59–72.
 - 25 Uefune F, Aonishi T, Kitaguchi T, Takahashi H, Seino S, Sakano D and Kume S (2022) Dopamine negatively regulates insulin secretion through activation of D1-D2 receptor heteromer. *Diabetes* **71**, 1946–1961.
 - 26 Asada A, Hayakawa H, Yanase N, Abe K, Sakurai F, Mizuguchi H and Urata Y (2018) A flow cytometry-based method to determine the titer of adenoviruses expressing an extraneous gene. *Biol Pharm Bull* **41**, 1615–1619.
 - 27 Niwa H, Yamamura K and Miyazaki J-I (1991) Efficient selection for high-expression transfectants with a novel eukaryotic vector. *Gene* **108**, 193–199.
 - 28 Schindelin J, Arganda-Carreras I, Frise E, Kaynig V, Longair M, Pietzsch T, Preibisch S, Rueden C, Saalfeld S, Schmid B *et al.* (2012) Fiji: an open-source platform for biological-image analysis. *Nat Methods* **9**, 676–682.
 - 29 Hatanaka M, Tanabe K, Yanai A, Ohta Y, Kondo M, Akiyama M, Shinoda K, Oka Y and Tanizawa Y (2011) Wolfram syndrome 1 gene (WFS1) product localizes to secretory granules and determines granule acidification in pancreatic beta-cells. *Hum Mol Genet* **20**, 1274–1284.
 - 30 Los GV, Encell LP, McDougall MG, Hartzell DD, Karassina N, Zimprich C, Wood MG, Learish R, Ohana RF, Urh M *et al.* (2008) HaloTag: a novel protein labeling technology for cell imaging and protein analysis. *ACS Chem Biol* **3**, 373–382.
 - 31 McClatchy DB, Martínez-Bartolomé S, Gao Y, Lavallée-Adam M and Yates JR (2020) Quantitative analysis of global protein stability rates in tissues. *Sci Rep* **10**, 1–12.
 - 32 Wu T, Zhang S, Xu J, Zhang Y, Sun T, Shao Y, Wang J, Tang W, Chen F and Han X (2020) Hrd1, an important player in pancreatic B-cell failure and therapeutic target for type 2 diabetic mice. *Diabetes* **69**, 940–953.
 - 33 Hu Y, Gao Y, Zhang M, Deng KY, Singh R, Tian Q, Gong Y, Pan Z, Liu Q, Boisclair YR *et al.* (2019) Endoplasmic reticulum-associated degradation (ERAD) has a critical role in supporting glucose-stimulated insulin secretion in pancreatic B-cells. *Diabetes* **68**, 733–746.
 - 34 Li N, Zhang S, Xiong F, Eizirik DL and Wang CY (2020) SUMOylation, a multifaceted regulatory mechanism in the pancreatic beta cells. *Semin Cell Dev Biol* **103**, 51–58.
 - 35 Corsa CAS, Pearson GL, Renberg A, Askar MM, Vozheiko T, MacDougald OA and Soleimanpour SA (2019) The E3 ubiquitin ligase parkin is dispensable for metabolic homeostasis in murine pancreatic β cells and adipocytes. *J Biol Chem* **294**, 7296–7307.
 - 36 Hoelen H, Zaldumbide A, Van Leeuwen WF, Torfs ECW, Engelse MA, Hassan C, Lebbink RJ, De Koning EJ, Rensing ME, De Ru AH *et al.* (2015) Proteasomal degradation of proinsulin requires Derlin-2, HRD1 and p97. *PLoS One* **10**, 1–16.
 - 37 Shrestha N, Liu T, Ji Y, Reinert RB, Torres M, Li X, Zhang M, Tang CHA, Hu CCA, Liu C *et al.* (2020) SellL-Hrd1 ER-associated degradation maintains β cell identity via TGF- β signaling. *J Clin Invest* **130**, 3499–3510.

Supporting information

Additional supporting information may be found online in the Supporting Information section at the end of the article.

Fig. S1. HEK293T cells express WFS1 endogenously at a much lower level compared to MIN6 cells.

Table S1. Primers used for generating WFS1 mutants.

Table S2. The WFS1 mutant vectors.